

# Mechanism of Dihydrogen Cleavage by High-Valent Metal Oxo Compounds: Experimental and Computational Studies

James P. Collman,<sup>\*,†</sup> LeGrande M. Slaughter,<sup>†</sup> Todd A. Eberspacher,<sup>†</sup>  
Thomas Strassner,<sup>‡</sup> and John I. Brauman<sup>†</sup>

Department of Chemistry, Stanford University, Stanford, California 94305-5080, and  
Institut für Anorganische Chemie, Technische Universität München, Lichtenbergstrasse 4,  
D-85747 Garching, Germany

Received June 18, 2001

The oxidation of dihydrogen by metal tetraoxo compounds was investigated. Kinetic measurements of the oxidations of H<sub>2</sub> by MnO<sub>4</sub><sup>−</sup> and RuO<sub>4</sub>, performed by UV–vis spectroscopy, showed these reactions to be quite rapid at 25 °C ( $k_1 \approx (3-6) \times 10^{-2} \text{ M}^{-1} \text{ s}^{-1}$ ). Rates measured for H<sub>2</sub> oxidation by MnO<sub>4</sub><sup>−</sup> in aqueous solution (using KMnO<sub>4</sub>) and in chlorobenzene (using <sup>n</sup>Bu<sub>4</sub>NMnO<sub>4</sub>) revealed only a minor solvent effect on the reaction rate. Substantial kinetic isotope effects [ $k_{\text{H}_2}/k_{\text{D}_2} = 3.8(2)$  (MnO<sub>4</sub><sup>−</sup>, aq), 4.5(5) (MnO<sub>4</sub><sup>−</sup>, C<sub>6</sub>H<sub>5</sub>Cl soln), and 1.8(6) (RuO<sub>4</sub>, CCl<sub>4</sub> soln)] indicated that H–H bond cleavage is rate determining and that the mechanism of dihydrogen cleavage is likely similar in aqueous and organic solutions. Third-row transition-metal oxo compounds, such as OsO<sub>4</sub>, ReO<sub>4</sub><sup>−</sup>, and MeReO<sub>3</sub>, were found to be completely unreactive toward H<sub>2</sub>. Experiments were performed to probe for a catalytic hydrogen/deuterium exchange between D<sub>2</sub> and H<sub>2</sub>O as possible evidence of dihydrogen  $\sigma$ -complex intermediates, but no H/D exchange was observed in the presence of various metal oxo compounds at various pH values. In addition, no inhibition of RuO<sub>4</sub>-catalyzed hydrocarbon oxidation by H<sub>2</sub> was observed. On the basis of the available evidence, a concerted mechanism for the cleavage of H<sub>2</sub> by metal tetraoxo compounds is proposed. Theoretical models were developed for pertinent MnO<sub>4</sub><sup>−</sup> + H<sub>2</sub> transition states using density functional theory in order to differentiate between concerted [2 + 2] and [3 + 2] scissions of H<sub>2</sub>. The density functional theory calculations strongly favor the [3 + 2] mechanism and show that the H<sub>2</sub> cleavage shares some mechanistic features with related hydrocarbon oxidation reactions. The calculated activation energy for the [3 + 2] pathway ( $\Delta H^\ddagger = 15.4 \text{ kcal mol}^{-1}$ ) is within 2 kcal mol<sup>−1</sup> of the experimental value.

## Introduction

Metal oxo functionalities are known or believed to be the active oxidants in a broad range of transition-metal-based systems capable of oxidizing carbon–hydrogen bonds, including biological monooxygenases such as the cytochromes P-450,<sup>1</sup> synthetic metalloporphyrin oxidation catalysts,<sup>2</sup> heterogeneous metal oxide catalysts,<sup>3</sup> and homogeneous inorganic oxidants such as permanganate and chromic acid.<sup>4,5</sup> However, despite a wealth of mechanistic studies on the various systems, no consistent mechanistic scheme unifying the modes of reactivity of these related classes of oxidants has emerged. The initial abstraction of a hydrogen radical has often been proposed as the key step in the oxidation of a C–H bond,<sup>5–8</sup> but conflicting

evidence has persisted, raising the possibility that polar (i.e., hydride transfer) or concerted mechanisms may be operating instead of or in addition to the radical pathway. Studies of the cytochrome P-450 oxidation systems are illustrative of these mechanistic ambiguities. The long-accepted “rebound mechanism”,<sup>6</sup> in which hydrogen atom abstraction by a ferryl moiety is followed by the collapse of the carbon radical to give a hydroxylated product, has been called into question by Newcomb and co-workers in a series of fast-radical clock studies.<sup>9</sup> These experiments suggested the plausibility of a “nonsynchronous concerted mechanism”, in which the carbon-based radical has a lifetime of only  $\sim 70$  fs and is best viewed as a fleeting component of the transition state ensemble rather than a true radical intermediate. In addition, evidence was found for a competing pathway involving carbocation intermediates.<sup>9d</sup> More recently, Shaik and co-workers have proposed that the mechanistic problems are best explained by considering two distinct reactive states of the iron oxo (one low-spin and one high-spin),<sup>10</sup> while Coon and co-workers have argued for the existence of multiple active oxidants in P-450 oxygenations, including iron peroxo and iron hydroperoxo species in addition

<sup>†</sup> Stanford University.

<sup>‡</sup> Technische Universität München.

- (1) (a) *Cytochrome P-450: Structure, Mechanism, and Biochemistry*; Ortiz de Montellano, P. R., Ed.; Plenum: New York, 1995. (b) Sono, M.; Roach, M. P.; Coulter, E. D.; Dawson, J. H. *Chem. Rev.* **1996**, 96, 2841–2887.
- (2) Meunier, B. *Chem. Rev.* **1992**, 92, 1411–1456.
- (3) *Structure–Activity and Selectivity Relationships in Heterogeneous Catalysis*; Grasselli, R. K., Sleight, A. W., Eds.; Elsevier: New York, 1991.
- (4) *Oxidation in Organic Chemistry*; Wiberg, K. B., Ed.; Academic Press: New York, 1965; Part A.
- (5) (a) Wiberg, K. B.; Evans, R. J. *Tetrahedron* **1960**, 8, 313. (b) Wiberg, K. B.; Foster, G. *Chem. Ind. (London)* **1961**, 108. (c) Wiberg, K. B.; Foster, G. *J. Am. Chem. Soc.* **1961**, 83, 423.
- (6) (a) Groves, J. T.; McCluskey, G. A. *J. Am. Chem. Soc.* **1976**, 98, 859–861. (b) Groves, J. T. *J. Chem. Educ.* **1985**, 62, 928–931.

(7) Brauman, J. I.; Pandell, A. J. *J. Am. Chem. Soc.* **1970**, 92, 329–335.

(8) Wiberg, K. B.; Fox, A. S. *J. Am. Chem. Soc.* **1963**, 85, 3487–3491.

(9) (a) Newcomb, M.; Le Tadic-Biadatti, M.-H.; Chestney, D. L.; Roberts, E. S.; Hollenberg, P. F. *J. Am. Chem. Soc.* **1995**, 117, 12085–12091. (b) Toy, P. H.; Newcomb, M.; Hollenberg, P. F. *J. Am. Chem. Soc.* **1998**, 120, 7719–7729. (c) Toy, P. H.; Dhanabalasingam, B.; Newcomb, M.; Hanna, I. H.; Hollenberg, P. F. *J. Org. Chem.* **1997**, 62, 9114–9122.

to ferryl intermediates.<sup>11</sup> Recent studies by our group<sup>12</sup> and others<sup>13</sup> on synthetic metalloporphyrin analogues of P-450 have also indicated that alternatives to the rebound mechanism must be considered. It is clear that a mechanistic understanding of metal oxo mediated oxidations remains incomplete and that any new evidence which adds to the current body of knowledge will be helpful.

Inorganic oxidants such as permanganate ( $\text{MnO}_4^-$ ) and ruthenium tetroxide ( $\text{RuO}_4$ ) are appealing models for the reactivity of metal oxo species. These well-defined homogeneous oxidants are capable of reacting with a wide variety of functional groups, including the C–H bonds of saturated and unsaturated hydrocarbons.<sup>14–18</sup> The metal tetraoxo compounds differ from the iron oxo intermediate in cytochrome P-450 in that they are closed-shell species, whereas the latter is known to possess a high-spin ground state; however, these compounds are still reasonable models for P-450 reactivity given that recent theoretical studies predict a lowest energy pathway for alkane hydroxylation which involves a low-spin state of the P-450 ferryl moiety.<sup>10</sup> Indeed, the reactivity patterns in these systems are quite similar to those observed in the P-450 enzymes and models (i.e., they exhibit radical-like selectivity in the oxidations of C–H bonds ( $3^\circ > 2^\circ > 1^\circ$ )), yet these reactions occur predominantly with retention of configuration.<sup>4,17–19</sup> Mayer and co-workers have recently published thorough studies of benzylic oxidations by permanganate<sup>15</sup> and  $\text{CrO}_2\text{Cl}_2$ <sup>16</sup> which showed that radical mechanisms appear to be operative in organic solvents, but a shift to a polar mechanism may occur upon changing to an aqueous solution.<sup>15a</sup> By contrast, a concerted C–H cleavage has been proposed for  $\text{RuO}_4$ -mediated hydroxylations of hydrocarbons on the basis of mechanistic investigations.<sup>18c–e</sup>

We were intrigued by decades-old reports of dihydrogen oxidation by permanganate<sup>20</sup> because we realized that this reaction has interesting implications for hydrocarbon oxidations by high-valent metal oxo species. The H–H bond of dihydrogen is approximately as strong as the C–H bond of methane, the

strongest among saturated hydrocarbons ( $\sim 105 \text{ kcal mol}^{-1}$ ),<sup>21</sup> and this would seem to preclude hydrogen atom abstraction as a mechanistic possibility. We have undertaken an examination of the reactions of permanganate and related metal oxo compounds with hydrogen in more detail in order to gain insights into the modes of reactivity of these oxidants. Herein are presented our experimental findings, including the first measurements of kinetic isotope effects (KIEs) for dihydrogen cleavage by metal oxo moieties and the first observations of dihydrogen oxidation by  $\text{RuO}_4$ . We also present a theoretical analysis which, together with our experimental results, suggests that a concerted bond cleavage is the most plausible first step in the oxidation of  $\text{H}_2$  by metal tetraoxo compounds.

## Experimental Section

**General Considerations.** Organic solvents (chlorobenzene and  $\text{CCl}_4$ ) were rigorously purified by the following procedure:<sup>22</sup> solvents were shaken with concentrated  $\text{H}_2\text{SO}_4$  until the washings were colorless, and then they were washed with  $\text{H}_2\text{O}$ , washed with aqueous  $\text{NaHCO}_3$ , dried over  $\text{CaCl}_2$ , and distilled from  $\text{P}_2\text{O}_5$ . The solvents were stored over activated 4 Å molecular sieves and were passed through a column of activated basic alumina immediately prior to use. Deionized water was purified by boiling with potassium permanganate for 24 h followed by distillation, and the purified water was stored under argon.

$\text{KMnO}_4$  (Aldrich, 99%),  $\text{KReO}_4$  (Strem, 99.9%),  $\text{MeReO}_3$  (Strem),  $\text{OsO}_4$  (Strem, 99.95%), and  $\text{RuCl}_3 \cdot x\text{H}_2\text{O}$  (Platina Laboratories, Inc., 41.3% Ru/wt) were used as obtained.  $^n\text{Bu}_4\text{NMnO}_4$  was prepared by a published procedure<sup>23</sup> and recrystallized from  $\text{CH}_2\text{Cl}_2/\text{Et}_2\text{O}$ . This material was stored at  $-20^\circ\text{C}$  in a sealed vial which was warmed to room temperature before opening. **Warning:**  $^n\text{Bu}_4\text{NMnO}_4$  has been reported to explode spontaneously<sup>23</sup> and should be handled carefully.  $\text{H}_2$  (Air Products, 99.995%) and  $\text{D}_2$  (CIL, 99.9%) were used without additional purification.

Gas chromatographic analyses were performed on a Hewlett-Packard 5890 instrument equipped with FID and TCD detectors. UV–vis spectra were recorded on a Hewlett-Packard 8452A diode array spectrometer. For kinetic experiments, the sample temperature was maintained at  $25^\circ\text{C}$  by the use of a thermostated cell holder connected to a Melsungen Thermomix 1441 water circulator. A Varian XL-400 spectrometer was used for NMR analyses.

**Kinetic Measurements:  $\text{MnO}_4^- + \text{H}_2$ .** An approximately 30 mM solution of  $\text{KMnO}_4$  in purified  $\text{H}_2\text{O}$  or  $^n\text{Bu}_4\text{NMnO}_4$  in  $\text{C}_6\text{H}_5\text{Cl}$  was prepared using an accurately measured sample of the permanganate salt, and an aliquot of this solution was diluted to 5 mL to give a 0.3 mM solution. This solution was placed in an apparatus consisting of a quartz cuvette connected to a 100 mL round-bottom flask and sealed with a Teflon stopcock. The solution was degassed on a vacuum line with stirring for  $\sim 20$  s at room temperature and then subjected to three freeze–pump–thaw degas cycles at  $-78^\circ\text{C}$ . After the solution was warmed to room temperature, the apparatus was opened to bubbling  $\text{H}_2$  or  $\text{D}_2$  at 1 atm while the solution was stirred for 1 min. The cuvette portion of the apparatus containing the solution was inserted into the thermostated cell holder of the spectrometer, and the temperature was allowed to equilibrate for 5 min before data collection commenced. UV–vis spectra were acquired at intervals of 180 s for 8–36 h, depending on the reaction rate. Three kinetic trials were performed for each substrate ( $\text{H}_2$  and  $\text{D}_2$ ). After the final spectra were recorded, solutions were analyzed using an iodometric UV–vis procedure<sup>24</sup> to determine the oxidation state of manganese.

- (10) (a) Shaik, S.; Filatov, M.; Schröder, D.; Schwartz, H. *Chem.–Eur. J.* **1998**, *4*, 193–199. (b) Ogliaro, F.; Harris, N.; Cohen, S.; Filatov, M.; de Visser, S. P.; Shaik, S. *J. Am. Chem. Soc.* **2000**, *122*, 8977–8989. (c) Schröder, D.; Shaik, S.; Schwarz, H. *Acc. Chem. Res.* **2000**, *33*, 139–145.
- (11) (a) Vaz, A. D. N.; Pernecky, S. J.; Raner, G. M.; Coon, M. J. *Proc. Natl. Acad. Sci. U.S.A.* **1996**, *93*, 4644–4648. (b) Toy, P. H.; Newcomb, M.; Coon, M. J.; Vaz, A. D. N. *J. Am. Chem. Soc.* **1998**, *120*, 9718–9719. (c) Newcomb, M.; Shen, R.; Choi, S.-Y.; Toy, P. H.; Hollenberg, P. F.; Vaz, A. D. N.; Coon, M. J. *J. Am. Chem. Soc.* **2000**, *122*, 2677–2686.
- (12) (a) Collman, J. P.; Chien, A. S.; Eberspacher, T. A.; Brauman, J. I. *J. Am. Chem. Soc.* **1998**, *120*, 425–426. (b) Collman, J. P.; Chien, A. S.; Eberspacher, T. A.; Brauman, J. I. *J. Am. Chem. Soc.* **2000**, *122*, 11098–11100.
- (13) (a) Nam, W.; Lim, M. H.; Lee, H. J.; Kim, C. *J. Am. Chem. Soc.* **2000**, *122*, 6641–6647. (b) Nam, W.; Lim, M. H.; Moon, S. K.; Kim, C. *J. Am. Chem. Soc.* **2000**, *122*, 10805–10809.
- (14) Stewart, R.; Spitzer, U. A. *Can. J. Chem.* **1978**, *56*, 1273–1279.
- (15) (a) Gardner, K. A.; Mayer, J. M. *Science* **1995**, *269*, 1849–1851. (b) Gardner, K. A.; Kuehnert, L. L.; Mayer, J. M. *Inorg. Chem.* **1997**, *36*, 2069–2078. (c) Mayer, J. M. *Acc. Chem. Res.* **1998**, *31*, 441–450.
- (16) (a) Cook, G. K.; Mayer, J. M. *J. Am. Chem. Soc.* **1994**, *116*, 1855–1868. (b) Cook, G. K.; Mayer, J. M. *J. Am. Chem. Soc.* **1995**, *117*, 7139–7156.
- (17) (a) Tenaglia, A.; Terranova, E.; Waegell, B. *Tetrahedron Lett.* **1989**, *30*, 5271–5274. (b) Tenaglia, A.; Terranova, E.; Waegell, B. *J. Chem. Soc., Chem. Commun.* **1990**, 1344–1345.
- (18) (a) Bakke, J. M.; Lundquist, M. *Acta Chem. Scand., Ser. B* **1986**, *40*, 430–433. (b) Bakke, J. M.; Brænden, J. E. *Acta Chem. Scand.* **1991**, *45*, 418–423. (c) Bakke, J. M.; Bethell, D. *Acta Chem. Scand.* **1992**, *46*, 644–649. (d) Bakke, J. M.; Frøhaug, A. E. *Acta Chem. Scand.* **1994**, *48*, 160–163. (e) Bakke, J. M.; Frøhaug, A. E. *J. Phys. Org. Chem.* **1996**, *9* (7), 507–513.
- (19) Groves, J. T.; Nemo, T. E. *J. Am. Chem. Soc.* **1983**, *105*, 6243–6248.

- (20) (a) Just, G.; Kauko, Y. Z. *Phys. Chem.* **1911**, *76*, 601–640. (b) Hein, F.; Daniel, W.; Schwedler, H. Z. *Anorg. Chem.* **1937**, *233*, 161–177. (c) Webster, A. H.; Halpern, J. *Trans. Faraday Soc.* **1957**, *53*, 51–60. (d) Halpern, J. *Adv. Catal.* **1957**, *9*, 302–311.
- (21) Berkowitz, J.; Ellison, G. B.; Gutman, D. *J. Phys. Chem.* **1994**, *98*, 2744–2765 and references therein.
- (22) Perrin, D. D.; Armarego, W. L. F. *Purification of Laboratory Chemicals*; Pergamon: New York, 1988.
- (23) Karaman, H.; Barton, R. J.; Robertson, B. E.; Lee, D. G. *J. Org. Chem.* **1984**, *49*, 4509–4518.

**Data Analysis:  $\text{MnO}_4^- + \text{H}_2$ .** Spectra were analyzed following a procedure described by Gardner et al.<sup>15b</sup> Absorbances were measured at 526 nm (a  $\text{MnO}_4^-$  absorption maximum) and at 494 nm (a reference wavelength where the colloidal  $\text{MnO}_2$  product absorbs strongly but  $\text{MnO}_4^-$  absorbs weakly), and these were used to calculate  $[\text{MnO}_4^-]$  at each point in time. Modeling of the scattering and absorption curve of  $\text{MnO}_2$  was required in order to obtain the ratio of effective extinction coefficients for  $\text{MnO}_2$  at the two different wavelengths; this was done separately for each kinetic run by performing a third-order polynomial fit of the absorbance versus wavelength data at  $\sim 2.5$  half-lives, with the region displaying residual  $\text{MnO}_4^-$  absorption (480–600 nm) omitted. Pseudo-first-order rate constants were calculated by nonlinear least-squares fitting of the  $[\text{MnO}_4^-]$  versus time data to the exponential form of the first-order rate law. Use of a different pair of wavelengths (548 and 450 nm) gave rates which were identical within experimental error. For the reaction in  $\text{C}_6\text{H}_5\text{Cl}$ , significant acceleration of the rate of  $\text{MnO}_4^-$  decay is seen at long reaction times, so only initial data were used to compute rate constants (30 min for  $\text{H}_2$  and 50 min for  $\text{D}_2$ ). These rates were corrected for the background solvent oxidation reaction ( $<9\%$ ). For the reaction in  $\text{H}_2\text{O}$ , no such acceleration was apparent, and the entire data range collected ( $\sim 2.5$  half-lives) was used in the rate calculation. Reported rates are average values for three separate runs for each substrate ( $\text{H}_2$  and  $\text{D}_2$ ), with uncertainties given at the 95% confidence level.<sup>25</sup>

Data were also analyzed using an alternative procedure based on the method of initial rates.<sup>26</sup> In this method, absorbance versus time data from the early stages of the reaction (30–50 min) were modeled using  $n$ th-order polynomial fits, and rate constants were calculated from averaged second coefficients ( $a_1$ ) for  $n = 4$  and 5. This method gave rates which differed by  $<10\%$  for the reaction in  $\text{C}_6\text{H}_5\text{Cl}$  but by 30–60% for the reaction in  $\text{H}_2\text{O}$ . In the latter case, the method appeared to suffer from interference by the  $\text{MnO}_2$  product early in the reaction because of the greater effective absorbance of  $\text{MnO}_2$  at low wavelengths in aqueous versus organic solutions. In addition, calculated uncertainties were large (e.g., 23% for  $\text{D}_2$  in  $\text{C}_6\text{H}_5\text{Cl}$  and 120% for  $\text{D}_2$  in  $\text{H}_2\text{O}$ ), and thus, only rates calculated by the previously described method are reported.

**Kinetic Measurements:  $\text{RuO}_4 + \text{H}_2$ .** A solution of  $\text{RuO}_4$  in  $\text{CCl}_4$  was prepared as follows. To a  $\sim 0.58$  mM solution of  $\text{RuCl}_3$  in 5 mL of  $\text{H}_2\text{O}$  were added 200 mg of  $\text{NaIO}_4$  and 5 mL of  $\text{CCl}_4$ . This biphasic mixture was stoppered and stirred vigorously for  $\sim 2$  h until the aqueous phase was colorless and the  $\text{CCl}_4$  phase was clear yellow. The  $\text{CCl}_4$  phase was then extracted by pipet and transferred to the sealable UV cell apparatus. UV-vis analysis indicated that  $>98\%$  of  $\text{RuCl}_3$  had been converted to  $\text{RuO}_4$  and extracted into the  $\text{CCl}_4$  phase. Even with rigorously purified  $\text{CCl}_4$ , a small amount of  $\text{RuO}_4$  decomposition ( $\sim 10\%$ ) was observed to occur over  $\sim 18$  h in the absence of substrate, apparently due to a trace impurity. Thus, solutions were incubated at room temperature for 24 h under  $\text{N}_2$  prior to the addition of  $\text{H}_2$  or  $\text{D}_2$ . Solutions were then degassed and exposed to  $\text{H}_2$  and  $\text{D}_2$  as described for the  $\text{MnO}_4^-$  experiments, and UV-vis data collection was started. Four separate kinetic runs were performed for  $\text{H}_2$  and six for  $\text{D}_2$ ; reported rate constants are average values, with errors given at the 95% confidence level.<sup>25</sup>

**Data Analysis:  $\text{RuO}_4 + \text{H}_2$ .** In the early stages of the reaction, absorbances at 310, 384, and 396 nm increased somewhat. This behavior was attributed to an initial buildup of colloidal  $\text{RuO}_2 \cdot x\text{H}_2\text{O}$  (vide infra), but after this initial period ( $\sim 2$  h), solid  $\text{RuO}_2$  particles began settling to the bottom of the cuvette, and the absorbances began uniformly decreasing. The absorbance at 310 nm was used to calculate rates because it was least affected by this phenomenon, and plots of Abs (310 nm) versus  $t$  after the initial period were modeled well by nonlinear least-squares fitting to a first-order exponential decay. Typically, data in the ranges of 130–300 min ( $\text{H}_2$ ) or 160–350 min ( $\text{D}_2$ ) were used.

**H/D Exchange Experiments. (a) Permanganate.** A solution of 40 mg of  $\text{KMnO}_4$  was prepared in 5 mL of deionized  $\text{H}_2\text{O}$  or an appropriate phosphate or carbonate buffer solution. The solution was placed in a 50 mL Schlenk flask fitted with a Suba-Seal septum and then degassed at room temperature and again at  $-78^\circ\text{C}$ . The solution was warmed, and 1 atm of  $\text{D}_2$  was admitted. The mixture was stirred for several days, and 10  $\mu\text{L}$  samples of headspace gas were periodically withdrawn by micropipet for GC analysis. A  $1/8$  in. GC column packed with  $\text{MnCl}_2$ -coated alumina and maintained at  $-196^\circ\text{C}$  was used to analyze for  $\text{H}_2$ , HD, and  $\text{D}_2$ ;<sup>27</sup> the column was connected to a heated cupric oxide column which converted hydrogen isotopologues to water vapor for TCD analysis.

**(b)  $\text{RuO}_4$ .** A catalytic biphasic  $\text{RuO}_4$  system was prepared in a 5 mL Schlenk flask by dissolving 8 mg of  $\text{RuCl}_3 \cdot x\text{H}_2\text{O}$  and 200 mg of  $\text{NaIO}_4$  in 2 mL of  $\text{H}_2\text{O}$  and then adding 1 mL of  $\text{CH}_3\text{CN}$  and 2 mL of  $\text{CCl}_4$ . The mixture was degassed, and  $\text{D}_2$  was admitted; GC analysis was performed as described previously.

**(c) Other Oxidants.** The 50 mM aqueous solutions were prepared in 50 mL Schlenk flasks as described for permanganate, and all of the other procedures were the same.

**NMR Tube Experiments.** Into a 5 mm NMR tube fitted with a poly(tetrafluoroethylene) valve was placed 8–10 mg of a transition-metal oxo compound.  $\text{D}_2\text{O}$  ( $\sim 0.7$  mL) was added, the tube was evacuated on a vacuum line while immersed in a cold water bath at  $\sim 3^\circ\text{C}$ , and 1 atm of  $\text{H}_2$  was admitted. The tube was sealed, stored at  $25^\circ\text{C}$ , and monitored periodically by  $^1\text{H}$  NMR.

**Kinetics of Adamantane Oxidation by  $\text{RuO}_4$ .** Reactions were performed using a modification of the catalytic conditions developed by Carlsen et al.<sup>18c,28</sup> Into each of two 100 mL Schlenk flasks were introduced 2.0 g of  $\text{NaIO}_4$ , 18 mL of  $\text{H}_2\text{O}$ , 10 mL of  $\text{CH}_3\text{CN}$ , and 20 mL of an 80 mM solution of adamantane in  $\text{CCl}_4$ , and the mixtures were stirred. The flasks were fitted with Suba-Seal septa and degassed; one flask was filled with Ar and the other with  $\text{H}_2$ . A total of 2.0 mL of a 0.16 M solution of  $\text{RuCl}_3$  was injected into each flask by syringe, and within a few minutes, brown  $\text{RuCl}_3$  had been converted to yellow  $\text{RuO}_4$  as monitored visually. The reaction was monitored using the following procedure. A 100  $\mu\text{L}$  aliquot of the organic (lower) layer was withdrawn by syringe and mixed with 3 mL of 3:1  $\text{PrOH}/\text{H}_2\text{O}$ , which reduced  $\text{RuO}_4$  to  $\text{RuO}_2$ . This mixture was extracted twice with 1 mL of  $\text{Et}_2\text{O}$  containing 1 mM *tert*-butyl benzene (external standard), and this extract was analyzed by GC. The two reactions were monitored in tandem over 48 h, and headspace gases were replaced periodically. Rates were calculated by fitting the adamantane concentration over time to a first-order exponential decay.

**Computational Details.** The density functional/Hartree-Fock hybrid model B3LYP,<sup>29,30</sup> as implemented in Gaussian 98,<sup>31</sup> was used throughout this study together with the triple- $\zeta$  basis set 6-311+G(d,p). This methodology has proven successful for the evaluation of flat potential energy surfaces (e.g., in examining hydrogen atom

- (24) Lee, D. G.; Perez-Benito, J. F. *J. Org. Chem.* **1988**, *53*, 5725–5728.  
 (25) Mendham, J.; Denney, R. C.; Barnes, J. D.; Thomas, M. *Vogel's Textbook of Quantitative Chemical Analysis*; Prentice Hall: New York, 2000; pp 127–128.  
 (26) (a) Chandler, W. D.; Lee, E. J.; Lee, D. G. *J. Chem. Educ.* **1987**, *64*, 878–881. (b) Laidler, K. J. *Chemical Kinetics*; McGraw-Hill: New York, 1965; pp 15–17.

- (27) (a) Yasumori, I.; Ohno, S. *Bull. Chem. Soc. Jpn.* **1966**, *39*, 1302–1306. (b) Collman, J. P.; Wagenknecht, P. S.; Lewis, N. S. *J. Am. Chem. Soc.* **1992**, *114*, 5665–5673.  
 (28) Carlsen, P. H. J.; Katsuki, T.; Martin, V. S.; Sharpless, K. B. *J. Org. Chem.* **1981**, *46*, 3936–3938.  
 (29) Lee, C.; Yang, W.; Parr, R. G. *Phys. Rev. B: Condens. Matter* **1988**, *37*, 785–789.  
 (30) (a) Becke, A. D. *J. Chem. Phys.* **1992**, *97*, 9173–9177. (b) Becke, A. D. *J. Chem. Phys.* **1993**, *98*, 1372–1377. (c) Becke, A. D. *J. Chem. Phys.* **1993**, *98*, 5648–5652.  
 (31) Frisch, M. J.; Trucks, G. W.; Schlegel, H. B.; Scuseria, G. E.; Robb, M. A.; Cheeseman, J. R.; Zakrzewski, V. G.; Montgomery, J. A., Jr.; Stratmann, R. E.; Burant, J. C.; Dapprich, S.; Millam, J. M.; Daniels, A. D.; Kudin, K. N.; Strain, M. C.; Farkas, O.; Tomasi, J.; Barone, V.; Cossi, M.; Cammi, R.; Mennucci, B.; Pomelli, C.; Adamo, C.; Clifford, S.; Ochterski, J.; Petersson, G. A.; Ayala, P. Y.; Cui, Q.; Morokuma, K.; Malick, D. K.; Rabuck, A. D.; Raghavachari, K.; Foresman, J. B.; Cioslowski, J.; Ortiz, J. V.; Stefanov, B. B.; Liu, G.; Liashenko, A.; Piskorz, P.; Komaromi, I.; Gomperts, R.; Martin, R. L.; Fox, D. J.; Keith, T.; Al-Laham, M. A.; Peng, C. Y.; Nanayakkara, A.; Gonzalez, C.; Challacombe, M.; Gill, P. M. W.; Johnson, B.; Chen, W.; Wong, M. W.; Andres, J. L.; Gonzalez, C.; Head-Gordon, M.; Replogle, E. S.; Pople, J. A. *Gaussian98*, Revision A.7; Gaussian, Inc.: Pittsburgh, PA, 1998.



abstraction by  $\text{MnO}_4^-$  from methane and toluene).<sup>32</sup> All of the geometries were fully optimized, and frequency calculations ensured that they corresponded to either minima (NIMAG 0) or transition states (NIMAG 1) on the potential energy surface. All of the energies listed are zero-point energy (ZPE) corrected and are given in kcal mol<sup>-1</sup> relative to the reactants. All of the values are unscaled. The stabilities of wave functions were checked, and unrestricted calculations ensured that no radical intermediates needed to be considered. Standard criteria were employed for self-consistent field (SCF) and convergence, with the maximum number of SCF cycles set to 250.

The calculated vibrational frequencies for transition states were used to compute KIEs according to Bigeleisen's treatment.<sup>33</sup> Plots were created using PLUTON.<sup>34</sup>

## Results

**Kinetic Studies and Isotope Effects.** Reaction rates and KIEs for the oxidation of  $\text{H}_2$  by metal oxo compounds were examined in this study as a means of gaining mechanistic insights into the  $\text{H}_2$  cleavage reaction. Kinetic data for the reaction of permanganate with  $\text{H}_2$  in water have been previously published,<sup>20c</sup> but no KIEs were reported. KIE measurements can provide information about the nature of the rate-determining step of a reaction and may allow different mechanisms to be distinguished by comparing KIEs for similar reactions.<sup>35</sup> Changes in the magnitude of a KIE upon switching solvents have been used to argue for a shift in mechanism in the oxidation of toluene by  $\text{MnO}_4^-$ ;<sup>15a</sup> thus, we examined the KIE for  $\text{H}_2$  oxidation by  $\text{MnO}_4^-$  in both aqueous and organic solutions.

The kinetics of the reactions of  $\text{H}_2$  and  $\text{D}_2$  with dilute solutions of  $\text{MnO}_4^-$  (0.3 mM) were measured at 25 °C by UV-vis spectroscopy. For the aqueous reactions,  $\text{KMnO}_4$  was used, and the water was rigorously purified to ensure that no oxidizable contaminants were present. No decrease in the UV-vis absorbance of aqueous  $\text{KMnO}_4$  solutions over time was detected in the absence of  $\text{H}_2$ . The tetrabutylammonium salt  $^n\text{Bu}_4\text{NMnO}_4$ <sup>23</sup> was employed in order to solubilize permanganate in organic solvents. Organic solvents with sufficient polarity to dissolve  $^n\text{Bu}_4\text{NMnO}_4$  are generally prone to oxidation; however, chlorobenzene ( $\text{C}_6\text{H}_5\text{Cl}$ ) was found to be a suitable solvent for these reactions because it is easily purified and reacts slowly with  $\text{MnO}_4^-$  relative to the reactions being studied (rates <9% of substrate oxidation).

In both  $\text{H}_2\text{O}$  and  $\text{C}_6\text{H}_5\text{Cl}$  solutions, the product of  $\text{MnO}_4^-$  reduction is colloidal  $\text{MnO}_2$ , which exhibits a diagnostic absorption and scattering spectrum.<sup>36</sup> Isosbestic points were observed in the UV-vis spectra during kinetic runs in both solvents, indicating that  $\text{MnO}_4^-$  and  $\text{MnO}_2$  are the only manganese-containing species present in significant concentrations. Oxidation state determinations for solutions near completion of the reaction (see Experimental Section) showed the average oxidation state of manganese to be 3.8(3). Thus, the balanced reaction for  $\text{H}_2$  oxidation by permanganate may be represented by eq 1. For the reaction in  $\text{C}_6\text{H}_5\text{Cl}$  solution, the  $\text{H}_2\text{O}$  and  $^n\text{Bu}_4\text{N}^+[\text{OH}^-]$  produced are probably associated with the  $\text{MnO}_2$  colloid.<sup>15b</sup> For the aqueous reaction, the use of a pH = 7 buffer resulted in no significant change in the rate compared with that of the unbuffered reaction, so the buildup of  $[\text{OH}^-]$  did not appear to affect the kinetic measurements.

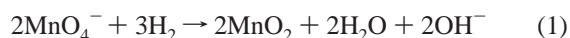


**Table 1.** Rates of  $\text{H}_2$  and  $\text{D}_2$  Oxidation by  $\text{MnO}_4^-$ <sup>a</sup>

solvent	sub- strate	$k_{\text{obs}}$ (s <sup>-1</sup> )	$[\text{H}_2/\text{D}_2]$ (mM) <sup>b</sup>	$k_2$ (M <sup>-1</sup> s <sup>-1</sup> )	KIE <sup>c</sup>
$\text{H}_2\text{O}$	$\text{H}_2$	$4.7(2) \times 10^{-5}$	0.781	$6.0(2) \times 10^{-2}$	3.8(2)
	$\text{D}_2$	$1.27(6) \times 10^{-5}$	0.808	$1.57(8) \times 10^{-2}$	
$\text{C}_6\text{H}_5\text{Cl}$	$\text{H}_2$	$7.6(8) \times 10^{-5}$	2.52	$3.0(3) \times 10^{-2}$	4.5(5)
	$\text{D}_2$	$1.69(8) \times 10^{-5}$	2.52 <sup>d</sup>	$6.7(3) \times 10^{-3}$	

<sup>a</sup> All of the data are reported for 25 °C and 1 atm of  $\text{H}_2$  or  $\text{D}_2$ . <sup>b</sup> Solubility data taken from ref 22. <sup>c</sup> Refers to  $k_{\text{H}_2}/k_{\text{D}_2}$ . <sup>d</sup> No solubility data available for  $\text{D}_2$  in  $\text{C}_6\text{H}_5\text{Cl}$ .

The rates of  $\text{H}_2$  and  $\text{D}_2$  oxidation by permanganate in both solvents are presented in Table 1. The second-order rate constants ( $k_2$ ), obtained by correcting for the solubility of the gaseous substrate in the respective solvents,<sup>37,38</sup> reveal a minor solvent effect, with the reaction proceeding approximately twice as fast in  $\text{H}_2\text{O}$  as in  $\text{C}_6\text{H}_5\text{Cl}$ . The rate data correspond to activation energies ( $\Delta G^\ddagger$ ) of 19.1 kcal mol<sup>-1</sup> for the aqueous reaction and 19.5 kcal mol<sup>-1</sup> for the reaction in  $\text{C}_6\text{H}_5\text{Cl}$ . The KIEs measured for the oxidation of  $\text{D}_2$  versus  $\text{H}_2$  are substantial and similar in magnitude for the two solvent systems studied:  $k_{\text{H}_2}/k_{\text{D}_2} = 3.8(2)$  in  $\text{H}_2\text{O}$  and 4.5(5) in  $\text{C}_6\text{H}_5\text{Cl}$ . The rates measured in  $\text{C}_6\text{H}_5\text{Cl}$  are reported as initial rates because the rate of disappearance of  $\text{MnO}_4^-$  was observed to increase as the reaction progressed. This may be due to the formation of solvent oxidation products or possibly oxidation products of the  $^n\text{Bu}_4\text{N}^+$  counterion,<sup>39</sup> which are susceptible to further oxidation by  $\text{MnO}_4^-$ . Similar rate accelerations have been reported in the oxidations of benzylic C-H bonds by  $^n\text{Bu}_4\text{NMnO}_4$  in organic solvents.<sup>15b</sup> The reactions in  $\text{H}_2\text{O}$  solvent showed clean pseudo-first-order behavior with no apparent acceleration over the entire range of data collected (~2.5 half-lives), so all of the data were used in the rate computation. Repeated measurements showed that the rates were reproducible, with maximum deviations from the mean of 3.1% in  $\text{H}_2\text{O}$  and 6.1% in  $\text{C}_6\text{H}_5\text{Cl}$ .

The reactivities of second- and third-row metal oxo species toward  $\text{H}_2$  were also explored. The following systems did not react with hydrogen over several days at room temperature:  $\text{KReO}_4$  in  $\text{H}_2\text{O}$ ,  $\text{MeReO}_3$  in  $\text{H}_2\text{O}$ ,  $\text{MeReO}_3$  in  $\text{C}_6\text{H}_6$ ,  $\text{OsO}_4$  in  $\text{H}_2\text{O}$ , and  $\text{OsO}_4$  in  $\text{CCl}_4$ .

However,  $\text{RuO}_4$  was found to readily oxidize  $\text{H}_2$ . Dilute  $\text{CCl}_4$  solutions of  $\text{RuO}_4$  (~0.5 mM) darkened to green upon initial exposure to  $\text{H}_2$ , and black  $\text{RuO}_2$  eventually began precipitating from the solution. Efforts to measure the rate of this reaction were complicated in the early stages of the reaction by the apparent formation of reduced ruthenium species, which absorbed more strongly than  $\text{RuO}_4$  in the 280–500 nm range of the UV-vis spectrum (see Experimental Section). The observed spectral changes and the green color of the solutions match the known properties of colloidal  $\text{RuO}_2 \cdot x\text{H}_2\text{O}$ .<sup>40</sup> Within ~2 h, the absorption and scattering spectrum of the colloid had disappeared, and solid  $\text{RuO}_2$  appeared to be the sole reduction

(35) Melander, L.; Saunders, W. H., Jr. *Reaction Rates of Isotopic Molecules*; Wiley: New York, 1980.

(36) Perez-Benito, J. F.; Arias, C. *J. Colloid Interface Sci.* **1992**, *152*, 70–84.

(37) *IUPAC Solubility Data Series: Hydrogen and Deuterium*; Young, C. L., Ed.; Pergamon Press: New York, 1981; Vol. 5/6, p 2 ( $\text{H}_2/\text{H}_2\text{O}$ ), pp 278–279 ( $\text{D}_2/\text{H}_2\text{O}$ ), pp 240–241 ( $\text{H}_2/\text{C}_6\text{H}_5\text{Cl}$ ), p 160 ( $\text{H}_2/\text{C}_6\text{H}_6$ ), p 287 ( $\text{D}_2/\text{C}_6\text{H}_6$ ), p 238 ( $\text{H}_2/\text{CCl}_4$ ), p 290 ( $\text{D}_2/\text{CCl}_4$ ).

(38) No solubility data are available for  $\text{D}_2$  in  $\text{C}_6\text{H}_5\text{Cl}$ . If  $\text{D}_2$  is assumed to be 2.5% more soluble than  $\text{H}_2$ , as is the case in  $\text{C}_6\text{H}_6$ ,<sup>37</sup> then the KIE for the oxidation of  $\text{H}_2/\text{D}_2$  by  $\text{MnO}_4^-$  in  $\text{C}_6\text{H}_5\text{Cl}$  increases to 4.6(5).

(39)  $\text{PhCOOH}$  has been observed as the product of the reaction of  $\text{MnO}_4^-$  with  $^n\text{Bu}_3(\text{PhCH}_2)\text{N}^+$ .<sup>15b</sup>

(40) Mills, A.; McMurray, N. *J. Chem. Soc., Faraday Trans. 1* **1988**, *84*, 379–390.

(32) Strassner, T.; Houk, K. N. *J. Am. Chem. Soc.* **2000**, *122*, 7821–7822.

(33) Bigeleisen, J. *J. Chem. Phys.* **1949**, *17*, 675–678.

(34) Spek, A. L. *PLUTON*; available from <http://www.cryst.chem.uu.nl/pluton>.

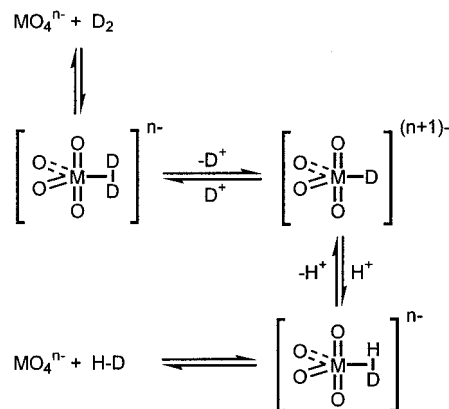
product; thus, rates were determined from the data collected beginning at 2.2–2.7 h into the reaction. The pseudo-first-order rate of  $\text{H}_2$  oxidation by  $\text{RuO}_4$  was measured to be  $8.2(17) \times 10^{-5} \text{ s}^{-1}$ . The rather poor reproducibility of the measured rates for four separate trials is reflected in the large uncertainty. The reproducibility of the  $\text{D}_2$  oxidation rates was even worse, but an average of six trials gives a rate of  $4.6(12) \times 10^{-5} \text{ s}^{-1}$ . The variation in rates may be due to the presence of varying amounts of water in the reaction mixtures or to heterogeneous effects related to the  $\text{RuO}_2$  product, and these effects are more pronounced in the slower  $\text{D}_2$  reaction.

The solubilities of  $\text{H}_2$  and  $\text{D}_2$  in  $\text{CCl}_4$  were corrected for (3.3 and 3.4 mM, respectively, at 1 atm/298 K),<sup>37</sup> and second-order rate constants of  $2.5(5) \times 10^{-2} \text{ M}^{-1} \text{ s}^{-1}$  for  $\text{H}_2$  and  $1.4(4) \times 10^{-2} \text{ M}^{-1} \text{ s}^{-1}$  for  $\text{D}_2$  were obtained; thus, the rates were very close to those of the corresponding  $\text{MnO}_4^-$  reactions. The KIE for the reaction is 1.8(6), but this value must be considered approximate in view of the reproducibility problems.

**H/D Exchange Experiments.** In the course of these kinetic studies, we recognized the possibility of dihydrogen  $\sigma$ -complex intermediates preceding bond cleavage. Previous studies of  $\text{H}_2$  oxidation by  $\text{MnO}_4^-$  predated the discovery of  $\text{H}_2$  complexes of transition metals,<sup>41</sup> so this possibility had not been considered. Such hydrogen adducts of high-valent metal oxo species are reasonable intermediates because amine adducts of  $\text{OsO}_4$  are well-known,<sup>42</sup> and kinetic evidence has been found for thioether complexes of  $\text{MnO}_4^-$  as intermediates in the oxidation of organic sulfides.<sup>43</sup>

As a probe for the existence of dihydrogen complexes of metal oxo compounds, we examined several systems for catalytic H/D exchange between  $\text{H}_2\text{O}$  solvent and  $\text{D}_2$ . This reaction, which is characteristic of a number of known dihydrogen complexes,<sup>44</sup> could occur via the loss of  $\text{D}^+$  from an acidic  $\text{D}_2$  complex followed by the protonation and release of  $\text{H}-\text{D}$  (Scheme 1). Such H/D exchange could also signify the existence of a metastable metal hydride intermediate.<sup>45</sup> In a typical permanganate experiment, a 50 mM solution of  $\text{KMnO}_4$  in  $\text{H}_2\text{O}$  was degassed and placed under 1 atm of  $\text{D}_2$ , and samples of gas were withdrawn periodically over several days for analysis using a cryogenic GC column capable of resolving  $\text{H}_2$ ,  $\text{HD}$ , and  $\text{D}_2$ .<sup>27</sup> The disappearance of the purple color of  $\text{MnO}_4^-$  and appearance of brown  $\text{MnO}_2$  indicated that permanganate was reduced by a reaction with  $\text{D}_2$ , but no traces of  $\text{HD}$  or  $\text{H}_2$  were detected. Some dihydrogen complexes exhibit maximum H/D exchange rates at a particular pH,<sup>44c,d</sup> a phenomenon which

Scheme 1



is also characteristic of the hydrogenase enzymes.<sup>46</sup> Therefore, the  $\text{KMnO}_4$  experiments were repeated at pH = 3.0, 5.5, 7.0, and 9.9, but still no H/D exchange was observed. The addition of 50 mM  $\text{Ag}^+$  (as  $\text{AgNO}_3$ ), which is known to catalyze the oxidation of  $\text{H}_2$  by  $\text{MnO}_4^-$ ,<sup>20b,c</sup> also did not result in detectable H/D exchange.

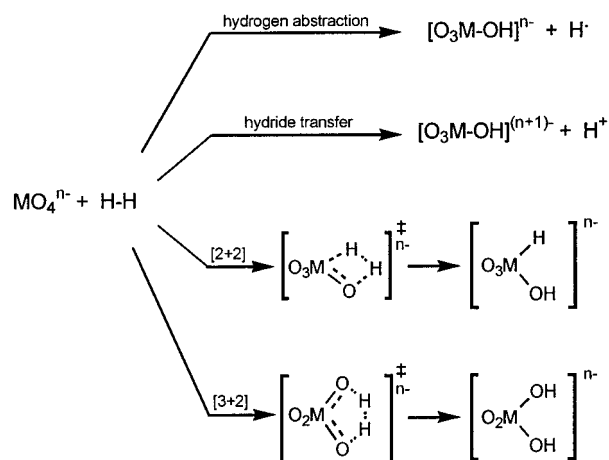
Because dihydrogen complexes of second- and third-row transition metals are known to be more stable than those of first-row metals,<sup>47</sup> the metal oxo species  $\text{RuO}_4$ ,  $\text{OsO}_4$ , and  $\text{ReO}_4^-$  as well as the related organometallic compound  $\text{MeReO}_3$  were examined for H/D exchange activity. For highly reactive  $\text{RuO}_4$ , a catalytic biphasic system<sup>18c,28</sup> was employed (see Experimental Section); for the other compounds, 50 mM aqueous solutions were used as in the  $\text{MnO}_4^-$  experiments. No H/D exchange was observed in these systems. In addition,  $\text{D}_2\text{O}$  solutions of  $\text{OsO}_4$ ,  $\text{KReO}_4$ , and  $\text{MeReO}_3$  under 1 atm of  $\text{H}_2$  were examined by  $^1\text{H}$  NMR for changes in the chemical shift or  $T_1$  of  $\text{H}_2$ , which would constitute evidence of an  $\text{H}_2$  complex, but no such changes were apparent.

**$\text{RuO}_4$ -Catalyzed Oxidation under  $\text{H}_2$ .** As a further test for the intermediacy of  $\text{H}_2$  complexes of metal oxos, the catalytic hydroxylation of adamantane was examined in the presence of  $\text{H}_2$ . The oxidation of adamantane is known to show clean kinetics over several half-lives,<sup>18c-e</sup> and the presence of an intermediate  $\text{H}_2$  complex of  $\text{RuO}_4$  in significant concentrations would be expected to inhibit hydrocarbon oxidation because of the sequestration of the active catalyst. Hydroxylation rates determined by monitoring the disappearance of adamantane in the presence of catalytic  $\text{RuO}_4$  under 1 atm of  $\text{H}_2$  and in the absence of  $\text{H}_2$  were identical ( $k_{\text{obs}} = 9.3(5) \times 10^{-6} \text{ s}^{-1}$  at 20 mol %  $\text{RuO}_4$ ; see Experimental Section). As previously reported,<sup>18c,d</sup> the major oxidation product was 1-adamantanol, with a small amount of 2-adamantanone (~2%) also produced. Because  $\text{RuO}_4$  reacts with  $\text{H}_2$  as well as adamantane (vide supra), the lack of inhibition indicates that reoxidation of reduced ruthenium species to  $\text{RuO}_4$  is not rate-limiting in the catalytic cycle and that an  $\text{H}_2$   $\sigma$ -complex intermediate is present in negligible concentrations or not at all.

- (41) (a) Kubas, G. J. *Acc. Chem. Res.* **1988**, *21*, 120–128. (b) Heinekey, D. M.; Oldham, W. J. *Chem. Rev.* **1993**, *93*, 913–926.  
 (42) (a) Criegee, R.; Marchand, B.; Wannowius, H. *Justus Liebigs Ann. Chem.* **1949**, *550*, 99. (b) Cleare, M. J.; Hydes, P. C.; Griffith, W. P.; Wright, M. J. *J. Chem. Soc., Dalton Trans.* **1977**, 941–944. (c) Griffith, W. P.; Skapski, A. C.; Woode, K. A.; Wright, M. J. *Inorg. Chim. Acta* **1978**, *31*, L413–L414. (d) Svendsen, J. S.; Markó, I.; Jacobsen, E. N.; Rao, C. P.; Bott, S.; Sharpless, K. B. *J. Org. Chem.* **1989**, *54*, 2263–2264. (e) Nelson, D. W.; Gypser, A.; Ho, P. T.; Kolb, H. C.; Kondo, T.; Kwong, H.-L.; McGrath, D. V.; Rubin, A. E.; Norrby, P.-O.; Gable, K. P.; Sharpless, K. B. *J. Am. Chem. Soc.* **1997**, *119*, 1840–1858.  
 (43) Xie, N.; Binstead, R. A.; Block, E.; Chandler, W. D.; Lee, D. G.; Meyer, T. J.; Thiruvazhi, M. *J. Org. Chem.* **2000**, *65*, 1008–1015.  
 (44) (a) Albeniz, A. C.; Heinekey, D. M.; Crabtree, R. H. *Inorg. Chem.* **1991**, *30*, 3632–3635. (b) Kubas, G. J.; Burns, C. J.; Khalsa, G. R. K.; Van Der Sluis, L. S.; Kiss, G.; Hoff, C. D. *Organometallics* **1992**, *11*, 3390–3404. (c) Collman, J. P.; Wagenknecht, P. S.; Hembre, R. T.; Lewis, N. T. *J. Am. Chem. Soc.* **1990**, *112*, 1294–1295. (d) Collman, J. P.; Wagenknecht, P. S.; Hutchison, J. E.; Lewis, N. S.; Lopez, M. A.; Guillard, R.; L'Her, M.; Bothner-By, A. A.; Mishra, P. K. *J. Am. Chem. Soc.* **1992**, *114*, 5654–5664.  
 (45) Stahl, S. S.; Labinger, J. A.; Bercaw, J. E. *J. Am. Chem. Soc.* **1996**, *118*, 5961–5976.

- (46) (a) Farkas, A.; Farkas, L.; Yudin, J. *Proc. R. Soc. London, Ser. A* **1934**, *B115*, 373. (b) Lospinat, P. A.; Berlier, Y.; Fauque, G.; Czechowski, M.; Dimon, B.; LeGall, J. *Biochimie* **1986**, *68*, 55–61. (c) Arp, D. J.; Burris, R. H. *Biochim. Biophys. Acta* **1982**, *700*, 7–15. (d) Teixeira, M.; Fauque, G.; Moura, I.; Lospinat, P. A.; Berlier, Y.; Prickril, B.; Peck, H. D.; Peck, H. D., Jr.; Xavier, A. V.; LeGall, J.; Moura, J. J. G. *Eur. J. Biochem.* **1987**, *167*, 47–58.  
 (47) Millar, J. M.; Kastrup, R. V.; Nelchior, M. T.; Horváth, I. T.; Hoff, C. D.; Crabtree, R. H. *J. Am. Chem. Soc.* **1990**, *112*, 9643–9645.

Scheme 2



## Discussion

**Mechanism of H<sub>2</sub> Cleavage.** The kinetic studies show that dihydrogen undergoes facile oxidation by MnO<sub>4</sub><sup>−</sup> and RuO<sub>4</sub> at room temperature, with activation energies (Δ*G*<sup>‡</sup>) of 19.1–19.5 kcal mol<sup>−1</sup> for MnO<sub>4</sub><sup>−</sup> and 19.6 kcal mol<sup>−1</sup> for RuO<sub>4</sub>. These reactions are faster than the oxidations of benzylic C–H bonds by permanganate<sup>15</sup> and the oxidations of tertiary C–H bonds of saturated hydrocarbons by RuO<sub>4</sub>.<sup>18</sup> The substantial KIEs observed for the dihydrogen oxidation reactions are consistent with a rate-determining step involving the cleavage of the H–H bond. The similarity of the KIEs for H<sub>2</sub> versus D<sub>2</sub> oxidation by MnO<sub>4</sub><sup>−</sup> in H<sub>2</sub>O and C<sub>6</sub>H<sub>5</sub>Cl solutions as well as the lack of an appreciable solvent effect on absolute reaction rates suggests a common mechanism in organic and aqueous solutions. The absence of catalytic H/D exchange in these systems and the lack of inhibition of hydrocarbon oxidation by H<sub>2</sub> indicate that dihydrogen complexes, at least, acidic ones, are unlikely intermediates.

In view of the unreactivity of third-row transition-metal oxo compounds such as OsO<sub>4</sub>, ReO<sub>4</sub><sup>−</sup>, and MeReO<sub>3</sub> toward dihydrogen, it is clear that MnO<sub>4</sub><sup>−</sup> and RuO<sub>4</sub> possess a special reactivity among metal tetraoxo compounds. It has been noted by Holm and co-workers<sup>48</sup> that greater thermodynamic stabilization of the higher oxidation states and stronger metal oxo bonds are two important factors contributing to the diminished reactivity of third-row versus second-row transition-metal oxo compounds.

Because the rate-determining H–H cleavage is the only kinetically accessible step in the oxidation of H<sub>2</sub> by MnO<sub>4</sub><sup>−</sup> and RuO<sub>4</sub>, the mechanistic discussion will focus on this bond scission event. Four plausible mechanisms for the reaction of H<sub>2</sub> with a metal oxo are shown in Scheme 2: (1) the abstraction of an H• radical, constituting a 1e<sup>−</sup> reduction of the metal, (2) hydride transfer, resulting in a 2e<sup>−</sup> reduction of the metal, (3) a concerted [2 + 2] addition across an M=O bond, with no change in the oxidation state of the metal, and (4) a concerted [3 + 2] addition involving two M=O functionalities, resulting in a 2e<sup>−</sup> reduction of the metal. Mechanisms involving an initial electron transfer to MnO<sub>4</sub><sup>−</sup> followed by bond cleavage, such as those that have been discussed for the oxidations of organic compounds by MnO<sub>4</sub><sup>−</sup>,<sup>49</sup> OsO<sub>4</sub>,<sup>50</sup> and oxometalloporphyrins,<sup>51</sup>

are precluded by the KIEs and lack of solvent dependence on rates and will not be considered here. Evaluation of the four mechanistic possibilities described above in light of the experimental evidence allows some of them to be discounted as implausible.

Hydrogen atom abstraction has been proposed for the MnO<sub>4</sub><sup>−</sup> oxidations of benzylic carbon–hydrogen bonds on the basis of a number of mechanistic studies.<sup>7,8,15</sup> The strongest evidence against a radical mechanism in the present case is simply that the oxidation of dihydrogen proceeds so rapidly. Compared with the oxidation of toluene by MnO<sub>4</sub><sup>−</sup>,<sup>15</sup> the reaction of H<sub>2</sub> with MnO<sub>4</sub><sup>−</sup> or RuO<sub>4</sub> is ~10<sup>5</sup> times faster. Because the H–H bond of dihydrogen (BDE = 104 kcal mol<sup>−1</sup>) is considerably stronger than the benzylic C–H bond of toluene (BDE = 92 kcal mol<sup>−1</sup>),<sup>21</sup> it is improbable that these reactions are both radical abstractions. Toluene is a special case among hydrocarbons in that benzylic stabilization of the radical may play a role, but this should make hydrogen abstraction more facile rather than slower relative to a more thermodynamically robust substrate such as hydrogen. Experimental data for free radicals such as •OH<sup>52,53</sup> and halogen atoms<sup>54</sup> show that the rates of hydrogen atom abstraction from H<sub>2</sub> are virtually identical (i.e., different by less than a factor of 5) to the rates of H• abstraction from CH<sub>4</sub>, which has a C–H bond comparable in strength to the H–H bond (BDE = 104.9 kcal mol<sup>−1</sup>).<sup>21</sup> By contrast, hydrogen abstraction from toluene by •OH occurs near the diffusion-controlled limit, 10<sup>2</sup>–10<sup>3</sup> times faster than the reaction of •OH with H<sub>2</sub>.<sup>55</sup> These data lead to the conclusion that bond strength is the primary influence on the activation energy in a simple radical abstraction rather than orbital differences between H–H and C–H bonds. Arguments correlating H• abstraction rates with a thermodynamic driving force, which were employed by Mayer and co-workers to argue for a radical mechanism in the reaction of MnO<sub>4</sub><sup>−</sup> with toluene,<sup>15</sup> would predict such a high activation energy for H• abstraction from H<sub>2</sub> that the reaction could not occur.<sup>56</sup>

Hydride transfer has been implicated in the MnO<sub>4</sub><sup>−</sup> oxidations of alcohols<sup>59</sup> and in the aqueous MnO<sub>4</sub><sup>−</sup> oxidation of toluene.<sup>15a</sup> However, a polar mechanism such as this would be expected

- (48) (a) Tucci, G. C.; Donahue, J. P.; Holm, R. H. *Inorg. Chem.* **1998**, *37*, 1602–1608. (b) Sung, K.-M.; Holm, R. H. *J. Am. Chem. Soc.* **2001**, *123*, 1931–1943.  
 (49) Wiberg, K. B.; Freeman, F. *J. Org. Chem.* **2000**, *65*, 573–576.  
 (50) Wallis, J. M.; Kochi, J. K. *J. Am. Chem. Soc.* **1988**, *110*, 8207–8223.

- (51) (a) Ostrovc, D.; Bruce, T. C. *Acc. Chem. Res.* **1992**, *25*, 314–320. (b) Kim, T.; Mirafzal, G. A.; Liu, J.; Bauld, N. L. *J. Am. Chem. Soc.* **1993**, *115*, 7653–7664. (c) Gross, Z.; Nimri, S. *J. Am. Chem. Soc.* **1995**, *117*, 8021–8022.  
 (52) For gas phase where (a) *k*(•OH + H<sub>2</sub>) = 3.5(2) × 10<sup>6</sup> M<sup>−1</sup> s<sup>−1</sup> (295 K), see: Overend, R. P.; Paraskevopoulos, G.; Cvetanovic, R. J. *Can. J. Chem.* **1975**, *53*, 3374–3382. For (b) *k*(•OH + CH<sub>4</sub>) = 3.4(3) × 10<sup>6</sup> M<sup>−1</sup> s<sup>−1</sup> (293 K), see: Dunlop, J. R.; Tully, F. P. *J. Phys. Chem.* **1993**, *97*, 11148–11150.  
 (53) For aqueous solution where *k*(•OH + H<sub>2</sub>) = 4.2 × 10<sup>7</sup> M<sup>−1</sup> s<sup>−1</sup> (298 K) and *k*(•OH + CH<sub>4</sub>) = 1.1 × 10<sup>8</sup> M<sup>−1</sup> s<sup>−1</sup> (298 K), see: Buxton, G. V.; Greenstock, C. L.; Helman, W. P.; Ross, A. B. *J. Phys. Chem. Ref. Data* **1988**, *17*, 513.  
 (54) For gas phase at 298 K where *k*(Cl• + H<sub>2</sub>) = 7.7 × 10<sup>6</sup> M<sup>−1</sup> s<sup>−1</sup>, *k*(Cl• + CH<sub>4</sub>) = 3.6 × 10<sup>7</sup> M<sup>−1</sup> s<sup>−1</sup>, *k*(Br• + H<sub>2</sub>) = 1.0 × 10<sup>−3</sup> M<sup>−1</sup> s<sup>−1</sup>, and *k*(Br• + CH<sub>4</sub>) = 2.2 × 10<sup>−3</sup> M<sup>−1</sup> s<sup>−1</sup>, see: Kerr, J. A. In *Selected Elementary Reactions*; Bamford, C. H., Tipper, C. F. H., Eds.; Comprehensive Chemical Kinetics 18; Elsevier: Amsterdam, 1976; pp 45–51.  
 (55) For aqueous solution where *k*(•OH + CH<sub>3</sub>Ph) = 3 × 10<sup>9</sup> M<sup>−1</sup> s<sup>−1</sup>.<sup>54</sup>  
 (56) The fitting of Mayer's data for benzylic hydrogen abstractions by <sup>99</sup>Bu<sub>4</sub>NMnO<sub>4</sub><sup>15b</sup> to the Polanyi relation Δ*G*<sup>‡</sup> = β + α(Δ*H*<sup>°</sup>)<sup>57</sup> and the extrapolation of the line to 24 kcal mol<sup>−1</sup> (Δ*H*<sup>°</sup> for MnO<sub>4</sub><sup>−</sup> + H<sub>2</sub> → O<sub>3</sub>MnOH<sup>−</sup> + H•, assuming *D*(MnO–H) = 80 kcal mol<sup>−1</sup>) gives *k*<sub>1</sub> ≈ 10<sup>−16</sup> M<sup>−1</sup> s<sup>−1</sup>. The actual rate constant should be even smaller because α → 1 for very endothermic reactions.<sup>58</sup>  
 (57) Evans, M. G.; Polanyi, M. *Trans. Faraday Soc.* **1936**, *32*, 1333–1360.  
 (58) Pross, A. *Theoretical and Physical Principles of Organic Reactivity*; Wiley: New York, 1995; pp 175–182.  
 (59) Stewart, R. *J. Am. Chem. Soc.* **1957**, *79*, 3057–3061.



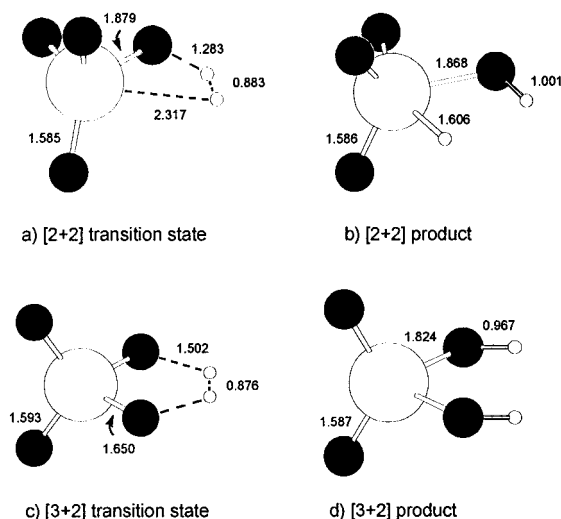


**Figure 1.** B3LYP/6-311+G\*\* transition states and products for  $\text{H}_2$  cleavage by  $\text{MnO}_4^-$ .

to give rise to a substantial solvent effect. In the present study of hydrogen oxidation by  $\text{MnO}_4^-$ , only a twofold increase in rate was observed on changing from  $\text{C}_6\text{H}_5\text{Cl}$  ( $\epsilon = 5.6$ ) to the much more polar solvent  $\text{H}_2\text{O}$  ( $\epsilon = 78.5$ ).

A concerted mechanism thus appears to fit the experimental evidence best. Concerted  $[2 + 2]$  addition of a C–H bond to a manganese oxo has been previously suggested for  $\text{MnO}_4^{2-}$  oxidations,<sup>60</sup> and a  $[3 + 2]$  mechanism has been proposed for the  $\text{RuO}_4$  oxidations of alkanes.<sup>18c–e</sup> Because the  $[3 + 2]$  and  $[2 + 2]$  addition pathways are kinetically indistinguishable, we turned to computational modeling in order to assess which of these mechanisms is more plausible for the oxidation of dihydrogen.

**Computational Studies.** The reaction of  $\text{H}_2$  with  $\text{MnO}_4^-$  was examined computationally using the hybrid density functional/Hartree–Fock model B3LYP<sup>29,30</sup> with the 6-311+G(d,p) basis set (see Experimental Section). This level of theory, which employs a large basis set with diffuse functions for improved modeling of anionic species, has been used successfully in studies of  $\text{MnO}_4^-$  reactions with alkenes<sup>61</sup> and toluene,<sup>32</sup> predicting activation enthalpies within 2 kcal mol<sup>−1</sup> of the experimental values.

Transition states and “products” were located for the two concerted pathways. The  $[2 + 2]$  addition transition state is characterized by a significant degree of O–H bond forming, with one O–H distance of 1.283 Å, and only a very weak interaction (2.317 Å) between the second hydrogen atom and the manganese center (Figure 1a). The manganese(VII) species resulting from the  $[2 + 2]$  addition,  $[\text{O}_3\text{Mn}(\text{OH})\text{H}]^-$  (Figure 1b), possesses a distorted trigonal-bipyramidal geometry, with the hydride and one oxo ligand occupying axial positions ( $\angle\text{O}_{\text{ax}}-\text{Mn}-\text{H} = 149.4^\circ$ ). The manganese hydride bond (1.606 Å) is significantly lengthened compared with the sum of the covalent radii (1.48 Å). The transition state for  $[3 + 2]$  addition shows a lesser degree of O–H bond forming (O–H distances 1.502 Å) but features a dissociating  $\text{H}_2$  unit which is symmetrically placed between two oxo functionalities (Figure 1c). The  $[3 + 2]$  addition step leads to the distorted tetrahedral manganese(V) species  $[\text{O}_2\text{Mn}(\text{OH})_2]^-$  (Figure 1d), which possesses two MnOH groups with an HO–Mn–OH angle of  $86.6^\circ$ .

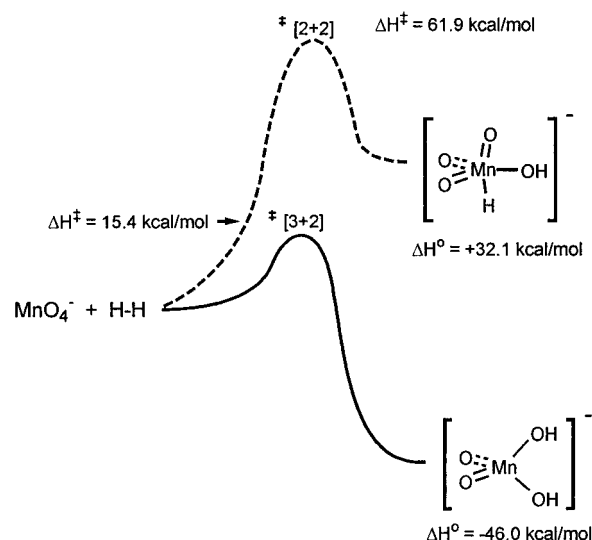


**Figure 2.** Calculated energy surfaces for  $[3 + 2]$  and  $[2 + 2]$  addition of  $\text{H}_2$  to  $\text{MnO}_4^-$ .

Optimized transition states were checked using unrestricted single-point calculations, and both the  $[2 + 2]$  and  $[3 + 2]$  transition states were calculated to lie on singlet energy surfaces. Vibrational analyses confirmed that each transition state possessed one imaginary frequency. No transition states leading to hydrogen atom or hydride abstraction were found. Furthermore, no intermediates preceding  $\text{H}_2$  cleavage (i.e.,  $\text{H}_2$   $\sigma$  complexes) were located along the reaction coordinates.

The computed energetics of the reaction are illustrated in Figure 2. The  $[3 + 2]$  addition is calculated to be exothermic by 46.0 kcal mol<sup>−1</sup>, while the  $[2 + 2]$  pathway is endothermic by 32.1 kcal mol<sup>−1</sup>. The calculated activation energies are 61.9 kcal mol<sup>−1</sup> for  $[2 + 2]$  addition and 15.4 kcal mol<sup>−1</sup> for  $[3 + 2]$  addition. The latter value compares favorably with the  $\Delta H^\ddagger$  of 14.0 kcal mol<sup>−1</sup> calculated from the rate data for the oxidation of  $\text{H}_2$  in  $\text{H}_2\text{O}$ .<sup>62</sup> Thus, the model predicts that  $[3 + 2]$  addition is strongly favored both kinetically and thermodynamically. This result can be rationalized by considering that the presence of multiple oxo ligands, which are strong  $\sigma$  and  $\pi$  donors, disfavors an increase in the coordination number of the manganese center. Given the similarity of the  $\text{H}_2$  oxidation rates for  $\text{MnO}_4^-$  and  $\text{RuO}_4$ , it is reasonable to propose that both reactions proceed by the same concerted mechanism. Calculations for  $\text{OsO}_4$  and  $\text{ReO}_4^-$  identify the  $[3 + 2]$  mechanism as the energetically favored pathway but predict significantly higher activation energies,<sup>63</sup> consistent with the experimentally observed lack of reactivity of these compounds toward  $\text{H}_2$ .

Parallels with the calculated energy surface for the carbon–hydrogen activation of toluene by  $\text{MnO}_4^-$  are noteworthy. The B3LYP-computed transition state for this reaction<sup>32</sup> clearly shows the involvement of two oxo groups, with one oxo forming an O–H bond and the other weakly interacting with the benzylic carbon of toluene. The transition state resembles a radical pair yet lies on a singlet energy surface. The collapse of the radical pair to give  $[\text{O}_2\text{Mn}(\text{OH})(\text{OCH}_2\text{Ph})]^-$  (the analogue of the  $[3 + 2]$  product in the reaction of  $\text{MnO}_4^-$  with  $\text{H}_2$ ) occurs with no barrier and no formation of free radicals. Experimental observa-

(60) Lee, D. G.; Chen, T. *J. Am. Chem. Soc.* **1993**, *115*, 11231–11236.

(61) (a) Houk, K. N.; Strassner, T. *J. Org. Chem.* **1999**, *64*, 800–802. (b) Strassner, T.; Busold, M. *J. Org. Chem.* **2001**, *66*, 672–676.

(62) Calculated using  $\Delta G^\ddagger = 19.1$  kcal mol<sup>−1</sup> from rate data in the present study and  $\Delta S^\ddagger = -17$  eu from Halpern's Eyring plot.<sup>20d</sup> The  $\Delta H^\ddagger$  for the reaction in  $\text{C}_6\text{H}_5\text{Cl}$  is calculated to be 14.4 kcal mol<sup>−1</sup> using the same  $\Delta S^\ddagger$  value, and Halpern's data for the aqueous reaction gave  $\Delta H^\ddagger = 13.8$  kcal mol<sup>−1</sup>.

(63) Strassner, T., paper in preparation.

tions of the partial loss of stereochemistry in benzylic oxidations by permanganate<sup>7,8</sup> can be explained by invoking the existence of a separate pathway for carbon-based radical dissociation from the singlet radical pair, which occurs at a finite rate. The toluene oxidation transition state is obviously related to the [3 + 2] transition state for the H<sub>2</sub> cleavage calculated in this study; the H<sub>2</sub> addition transition state is "earlier" and more symmetric by virtue of the greater exothermicity of the reaction and the potential to form two MnO–H bonds. These differences result in a purely concerted mechanism for the H–H activation, while the benzylic C–H activation proceeds by a more asynchronous mechanism resembling a hydrogen abstraction/oxygen rebound, though the essential features of the two reactions are similar.

**KIE Magnitudes.** The KIEs of 3.8–4.5 for H<sub>2</sub> versus D<sub>2</sub> oxidation by MnO<sub>4</sub><sup>−</sup> are substantial.<sup>64</sup> The largest published KIE for a related solution-phase reaction is 2.5, measured for the hydrogenolysis of the neopentyl ligand of (C<sub>5</sub>Me<sub>5</sub>)<sub>2</sub>Th(CH<sub>2</sub>–CMe<sub>3</sub>)(OCH<sub>2</sub>CMe<sub>3</sub>).<sup>72</sup> Typical KIEs for the oxidative addition of H<sub>2</sub> to coordinatively unsaturated metal centers are smaller, usually falling in the range 1.05–1.5.<sup>73</sup> The reported KIE for the gas-phase reaction of •OH radicals with H<sub>2</sub>/D<sub>2</sub> is 2.6.<sup>74</sup>

Large primary KIEs are typically attributed to two factors:<sup>75</sup> (1) similar degrees of bond formation and bond breakage in the transition state and (2) the linear transfer of a hydrogen atom. The energetically favored [3 + 2] addition transition state for MnO<sub>4</sub><sup>−</sup> + H<sub>2</sub> is relatively early ( $r(\text{H}–\text{H}) = 0.876 \text{ \AA}$ ) for the computational model employed in this study and does not feature linear hydrogen transfer. However, the reaction of interest

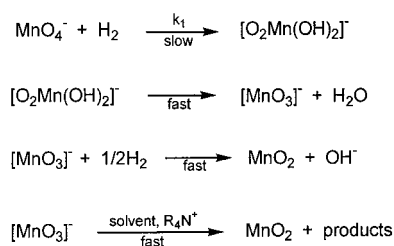
involves the transfer of *two* hydrogen atoms rather than just one, so it is reasonable to question the validity of standard rationalizations of KIE magnitudes on the basis of simple three-atom models<sup>75</sup> in this case.

We examined the KIE for H<sub>2</sub>/D<sub>2</sub> activation by MnO<sub>4</sub><sup>−</sup> using our computational model. Calculated vibrational frequencies for the H<sub>2</sub> [3 + 2] addition transition state and the D<sub>2</sub> analogue<sup>76</sup> yielded a calculated KIE of 1.63,<sup>77</sup> considerably lower than the experimentally measured values. Even the use of a frequency scale factor of 0.9, such as has been commonly employed to make Hartree–Fock-computed frequencies more realistic,<sup>80,81</sup> only increased the calculated KIE to 2.34, still in poor agreement with experiment. The discrepancy could result from a systematic error in the calculations, for example, poor modeling of low-frequency isotopically sensitive vibrations.<sup>83</sup> No significant problems are apparent in the analysis of the experimental rate data, and the use of an alternative method of rate calculation gave similar KIE values.<sup>84</sup> Another possible explanation for the disparity is tunneling, which has most notably been invoked to account for extraordinarily large KIEs of 20–50 in enzymatic C–H activations<sup>85,86</sup> but has also been used to explain H<sub>2</sub> addition KIEs which were only moderately larger than those predicted by classical models.<sup>73c</sup> Application of the standard Wigner correction<sup>87</sup> with the unscaled frequencies results in a small but significant increase of the calculated KIE to 2.20. This correction is based on an X–H–Y situation in the transition state, and it is conceivable that the unusual X–H–H–Y configuration in the [3 + 2] transition state might give rise to a larger tunnel effect. However, pending the development of

- (64) KIEs for H<sub>2</sub>/D<sub>2</sub> cleavages are generally significantly smaller than those for the corresponding C–H/C–D scissions. Several examples of metal-mediated C–H activation KIEs with magnitudes of 8–13 have been reported.<sup>7,15a,19,65–69</sup>
- (65) A theoretical study by Abu-Hasanayn et al.<sup>70</sup> suggested that the small magnitudes of H<sub>2</sub>/D<sub>2</sub> cleavage KIEs are due to the appearance of five new isotopically sensitive vibrational modes in the transition state relative to free H<sub>2</sub>. These vibrations produce significant inverse (<1) EXC and ZPE factors which compensate for the large H<sub>2</sub>/D<sub>2</sub> mass moment of inertia (MMI) term of ~5.7. Early transition states have also been invoked to explain the small KIEs.<sup>71</sup>
- (66) (a) Hjelmeland, L. M.; Aronow, L.; Trudell, J. R. *Biochem. Biophys. Res. Commun.* **1977**, *76*, 541–549. (b) Groves, J. T.; McCluskey, G. A.; White, R. E.; Coon, M. J. *Biochem. Biophys. Res. Commun.* **1978**, *81*, 154–160. (c) Miwa, G. T.; Walsh, J. S.; Lu, A. Y. H. *J. Biol. Chem.* **1984**, *259*, 3000–3004. (d) Lindsay-Smith, J. R.; Sleath, P. R. *J. Chem. Soc., Perkin Trans. 2* **1983**, 621–628. (e) Jones, J. P.; Korzekwa, K. R.; Rettie, A. E.; Trager, W. F. *J. Am. Chem. Soc.* **1986**, *108*, 7074–7078. (f) Jones, J. P.; Trager, W. F. *J. Am. Chem. Soc.* **1987**, *109*, 2171–2173. (g) Jones, J. P.; Trager, W. F. *J. Am. Chem. Soc.* **1988**, *110*, 2018. (h) Jones, J. P.; Rettie, A. E.; Trager, W. F. *J. Med. Chem.* **1990**, *33*, 1242–1246.
- (67) (a) Nappa, M. J.; McKinney, R. J. *Inorg. Chem.* **1988**, *27*, 3740–3745. (b) Sorokin, A. B.; Khenkin, A. M. *J. Chem. Soc., Chem. Commun.* **1990**, 45–46. (c) Sorokin, A.; Robert, A.; Meunier, B. *J. Am. Chem. Soc.* **1993**, *115*, 7293–7299.
- (68) Wayland, B. B.; Ba, S.; Sherry, A. E. *J. Am. Chem. Soc.* **1991**, *113*, 5305–5311.
- (69) Schaller, C. P.; Cummins, C. C.; Wolczanski, P. T. *J. Am. Chem. Soc.* **1996**, *118*, 591–611.
- (70) Abu-Hasanayn, F.; Goldman, A. S.; Krogh-Jespersen, K. *J. Phys. Chem.* **1993**, *97*, 5890–5896.
- (71) Collman, J. P.; Roper, W. R. *Adv. Organomet. Chem.* **1967**, *7*, 53–94.
- (72) Lin, Z.; Marks, T. J. *J. Am. Chem. Soc.* **1987**, *109*, 7979–7985.
- (73) (a) Chock, P. B.; Halpern, J. *J. Am. Chem. Soc.* **1966**, *88*, 3511. (b) Vaska, L.; Wernecke, F. *Trans. N.Y. Acad. Sci.* **1971**, *33*, 70. (c) Zhou, P.; Vitale, A. A.; San Filippo, J.; Saunders, W. H. *J. Am. Chem. Soc.* **1985**, *107*, 8049–8054. (d) Bullock, R. M. In *Transition Metal Hydrides*; Dedieu, A., Ed.; VCH: New York, 1992; pp 263–307.
- (74) Paraskevopoulos, G.; Nip, W. S. *Can. J. Chem.* **1980**, *58*, 2146–2149.
- (75) (a) Lowry, T. H.; Richardson, K. S. *Mechanism and Theory in Organic Chemistry*; Harper & Row: New York, 1987; pp 236–238. (b) Carpenter, B. K. *Determination of Organic Reaction Mechanisms*; Wiley: New York, 1984; pp 83–111.

- (76) Experimental frequencies were used for H<sub>2</sub> (4395 cm<sup>−1</sup>) and D<sub>2</sub> (3118 cm<sup>−1</sup>). Moelwyn-Hughes, E. A. *Physical Chemistry*; Pergamon Press: New York, 1961; p 427.
- (77) The same value is obtained using either the Bigeleisen expression<sup>33</sup> or the Redlich–Teller product rule.<sup>78</sup> The factored energetic contributions (KIE = MMI × EXC × ZPE) are as follows: MMI = 5.07, EXC = 0.78, ZPE = 0.41. A previous study of equilibrium isotope effects for hydrocarbon addition<sup>79</sup> has shown that large substrate MMI terms are effectively canceled by inverse EXC and ZPE factors from "new" isotopically sensitive vibrational modes appearing upon substrate binding or activation, which correspond to remnants of free substrate rotation and translation. Accordingly, new isotopically sensitive vibrations in the [3 + 2] H<sub>2</sub> addition transition state account for the entire EXC term of 0.78 and a factor of 0.11 in the ZPE term, leaving a ZPE factor of 3.75 from the weakened H–H stretch.
- (78) Schaad, L. J.; Bytautas, L.; Houk, K. N. *Can. J. Chem.* **1999**, *77*, 875–878.
- (79) Slaughter, L. M.; Wolczanski, P. T.; Klinckman, T. R.; Cundari, T. R. *J. Am. Chem. Soc.* **2000**, *122*, 7953–7975.
- (80) (a) Flock, M.; Ramek, M. *Int. J. Quantum Chem.* **1993**, *27*, 331–336. (b) Harris, N. J. *J. Phys. Chem.* **1995**, *99*, 14689–14699. (c) Cundari, T. R.; Raby, P. D. *J. Phys. Chem.* **1997**, *101*, 5783–5788.
- (81) Frequency scale factors required to bring density functional theory calculated frequencies into close agreement with the experiment are generally very close to unity,<sup>82</sup> and thus, these frequencies are typically reported unscaled.
- (82) Rauhut, G.; Pulay, P. *J. Phys. Chem.* **1995**, *99*, 3093–3100.
- (83) According to the density functional theory model, low-frequency vibrations result in strongly inverse EXC and ZPE factors which overcompensate for the large MMI term (see ref 77).
- (84) Initial rates calculated by polynomial fitting of Abs versus time data<sup>26</sup> (see Experimental Section) gave KIEs of 4.3 for C<sub>6</sub>H<sub>5</sub>Cl solution and 3.1 for aqueous solution, though the calculated uncertainties were large (35% and 55%, respectively).
- (85) (a) Nesheim, J. C.; Lipscomb, J. D. *Biochemistry* **1996**, *35*, 10240–10247. (b) Valentine, A. M.; Stahl, S. S.; Lippard, S. J. *J. Am. Chem. Soc.* **1999**, *121*, 3876–3887.
- (86) (a) Glickman, M. H.; Wiseman, J. S.; Klinman, J. P. *J. Am. Chem. Soc.* **1994**, *116*, 793–794. (b) Glickman, M. H.; Klinman, J. P. *Biochemistry* **1995**, *34*, 14077–14092. (c) Hwang, C.-C.; Grissom, C. B. *J. Am. Chem. Soc.* **1994**, *116*, 795–796. (d) Lewis, E. R.; Johansen, E.; Holman, T. R. *J. Am. Chem. Soc.* **1999**, *121*, 1395–1396.
- (87) (a) Wigner, E. Z. *Phys. Chem., Abt. B* **1932**, *19*, 203. (b) Bell, R. P. *Tunnel Effect in Chemistry*; Chapman & Hall: New York, 1980.



**Scheme 3**

an appropriate tunneling model, it is best to consider the origin of the unusually large measured KIEs as an open question. The excellent agreement between the experimental and calculated activation energies still strongly favors the [3 + 2] addition mechanism.

**Overall Reaction.** Assuming that the rate-determining H–H cleavage is a [3 + 2] addition, the overall reaction of  $\text{MnO}_4^-$  with  $\text{H}_2$  to give  $\text{MnO}_2$  and  $\text{H}_2\text{O}$  may be represented by the sequence of reactions in Scheme 3. The product of the first step is the manganese(V) intermediate  $[\text{O}_2\text{Mn}(\text{OH})_2]^-$ , which could rapidly lose water to yield  $\text{MnO}_3^-$ . Manganese(V) species of this type are known to be extremely reactive,<sup>88</sup> and this intermediate would readily oxidize another equivalent of  $\text{H}_2$ , the solvent, or a  $^n\text{Bu}_4\text{N}^+$  counterion.<sup>39</sup> The latter two reactions might lead to the formation of species which would react rapidly with  $\text{MnO}_4^-$ , accounting for the rate acceleration observed in the  $\text{C}_6\text{H}_5\text{Cl}$  solution. The  $\text{RuO}_4$  reaction might proceed by an analogous series of steps, with an  $\text{RuO}_3$  intermediate rapidly oxidizing a second equivalent of  $\text{H}_2$  to give the observed  $\text{RuO}_2$  product.

**Conclusions**

We have examined the oxidation of dihydrogen by  $\text{MnO}_4^-$  and other high-valent metal oxo compounds in order to gain insights into the mechanism of this unusual reaction. The rapid reaction rates and lack of significant solvent effects argue against radical or hydride abstraction mechanisms, and computational modeling of the  $\text{MnO}_4^-$  reaction supports a concerted [3 + 2] addition of  $\text{H}_2$  involving two oxo ligands. The KIEs measured

for the oxidation of  $\text{H}_2$  by  $\text{MnO}_4^-$  and  $\text{RuO}_4$  implicate a rate-determining H–H cleavage, though the origins of the large KIE magnitudes of 3.8–4.5 for the  $\text{MnO}_4^-$  reactions remain unclear.

Though the rates of  $\text{H}_2$  oxidation by the high-valent metal oxos studied here are much faster than those of the corresponding oxidations of C–H bonds, similarities in the B3LYP-calculated energy surfaces for these reactions, coupled with the success of these models in predicting activation energies, offer hope that a unified mechanistic picture can be devised which encompasses both  $\text{H}_2$  and hydrocarbon activations. The concerted [3 + 2] addition characteristic of  $\text{H}_2$  cleavage can be transformed into a C–H activation mechanism resembling hydrogen atom abstraction by replacing one O–H interaction with a very weak O–C interaction in the transition state and increasing the degree of bond forming in the other O–H interaction. While one oxo group rather than two is presumed to be involved in cytochrome P450-type metalloporphyrin-catalyzed oxidations, the nonsynchronous concerted mechanism, which has recently been proposed as an alternative to the radical abstraction/oxygen rebound mechanism in these systems,<sup>9</sup> is clearly related to the asynchronous mechanism of C–H activation of toluene by  $\text{MnO}_4^-$ . Considered together with these hydrocarbon activation reactions, the concerted reaction of  $\text{H}_2$  with  $\text{MnO}_4^-$  and  $\text{RuO}_4$  adds to the growing body of evidence which suggests that a more sophisticated mechanistic description is required for metal oxo mediated oxidations than simple, stepwise hydrogen abstraction.

**Acknowledgment.** We gratefully acknowledge the NSF (Grant No. CHE9612725) for financial support of this research. T.S. thanks Prof. Wolfgang Hermann (TUM) for research support and the Leibniz-Rechenzentrum München for computer time.

**Supporting Information Available:** Representative kinetic plots for  $\text{H}_2$  oxidation by  $\text{MnO}_4^-$  (in  $\text{H}_2\text{O}$  and  $\text{C}_6\text{H}_5\text{Cl}$ ) and by  $\text{RuO}_4$  (in  $\text{CCl}_4$ ); Gaussian98 archive files for calculated  $\text{H}_2 + \text{MnO}_4^-$  transition states and products, containing optimized geometries and thermochemical outputs; and assignments of calculated vibrational modes for  $\text{H}_2/\text{D}_2 + \text{MnO}_4^-$  [3 + 2] addition transition states. This material is available free of charge via the Internet at <http://pubs.acs.org>.

IC010639J

(88) Zahonyi-Budo, E.; Simandi, L. I. *Inorg. Chim. Acta* **1996**, *248*, 81–84.